이학석사학위논문

Reactive oxygen species promote heat shock protein 90-mediated HBV capsid assembly

활성산소는 열 충격 단백질 90이 매개하는 HBV 캡시드 조립을 촉진시킨다

2015 년 8 월

서울대학교 대학원

생명과학부

김윤식

이학석사학위논문

Reactive oxygen species promote heat shock protein 90-mediated HBV capsid assembly

활성산소는 열 충격 단백질 90이 매개하는 HBV 캡시드 조립을 촉진시킨다

2015 년 8 월

서울대학교 대학원

생명과학부

김윤식

Reactive oxygen species promote heat shock protein 90-mediated HBV capsid assembly

활성산소는 열 충격 단백질 90이 매개하는 HBV 캡시드 조립을 촉진시킨다

지도교수 정 구 흥

이 논문을 이학석사학위논문으로 제출함

2015년 8월

서울대학교 대학원

생명과학부

김윤식

김윤식의 석사학위논문을 인준함

2015년 8월

위 원 장_____(인)

부 위 원 장_____(인)

위 원_____(인)

Abstract

Reactive oxygen species promote heat shock protein 90-mediated HBV capsid assembly

Yoon Sik Kim
Life science
The Graduate School
Seoul National University

Hepatitis B virus (HBV) infection induces reactive oxygen species (ROS) production and has been associated with the development of hepatocellular carcinoma (HCC). ROS are also an important factor in HCC because the accumulated ROS leads to abnormal cell proliferation and chromosome mutation. In oxidative stress, heat shock protein 90 (Hsp90) and glutathione (GSH) function as part of the defense mechanism. Hsp90 prevents cellular component from oxidative stress, and GSH acts as antioxidants scavenging ROS in the cell. However, it is not known whether molecules regulated by oxidative stress are involved in HBV capsid assembly. Based on the previous study that Hsp90 facilitates HBV capsid assembly, which is an important step for the packing of viral particles, here, we show that ROS enrich Hsp90-driven HBV capsid formation. In cell-free system, HBV capsid assembly was facilitated by ROS with Hsp90, whereas it was decreased without Hsp90. In addition, GSH inhibited the

function of Hsp90 to decrease HBV capsid assembly. Consistent with the result of cell-free system, ROS and buthionine sulfoximine (BS), an inhibitor of GSH synthesis, increased HBV capsid formation in HepG2.2.15 cells. Thus, our study uncovers the interplay between ROS and Hsp90 during HBV capsid assembly.

Keywords: Hepatitis B virus; Capsid assembly; Core protein 149; Reactive oxygen species; Heat shock protein 90; Glutathione

Student Number: 2012-23060

Content

List of abbreviations

NAC	N-acetyl-L-cysteine
qPCR	Quantitative PCR
CD	Circular dichroism
H_2O_2	Hydrogen peroxide
GSH	Reduced glutathione

Introduction

Hepatitis B virus (HBV), a member of the hepadnaviridae family, has infected over two billion people worldwide [1]. Approximately 240 million HBsAg-positive individuals remain chronically infected and chronic HBV infection is associated with liver disease, including the development of hepatocellular carcinoma (HCC) and liver cirrhosis [1,2]. HBV generates reactive oxygen species (ROS) through altering mitochondrial function, and ROS can affect viruses by changing the redox state of the cell and by activating transcription factors such as NF-kB, which elevates the level of viral replication [3,4,5].

HBV has a partially double-stranded DNA genome consisting of four open reading frames (ORF), denoted Cp (core protein), Sp (surface protein), Pol (polymerase), and HBx (X protein) [6]. Following the infection of hepatocytes, the HBV genome is converted into covalently closed circular DNA (cccDNA) by a DNA repair system in the nucleus [7]. Subsequently, pregenomic RNA (pgRNA) is produced from host RNA polymerase, and it is packaged from the core protein with polymerase and other components such as host factors in the cytoplasm.

One of the host factors for HBV capsid formation is heat shock protein 90 (Hsp90). Hsp90 is activated by p23 and ATP to form the Hsp90 complex facilitating maturation of client protein [8], and the activated Hsp90 facilitates HBV capsid assembly in encapsidation [9]. Moreover, Hsp90 is associated with oxidative stress. In oxidative stress, ROS influences Hsp90 protecting activated 20S proteasomes to promote degradation of oxidized substrates [10].

Cells continuously produce ROS, which induce oxidative stress and are neutralized by antioxidant systems, as part of the metabolic process [11]. A low level of ROS is essential in several physiologic processes of the cell including proliferation, apoptosis, cell cycle arrest, etc [12]. At high ROS level, however, ROS causes oxidative stress and a toxic environment to the cells [13]. This stressful condition is known to play a

major role in HCC mainly by enhancing DNA damage and by modifying some key cellular process for development [13].

Virus-induced ROS have an effect not only on infected cells but also on the virus itself. Based on the previous study that HBV-induced ROS can cause HCC [3,4,14] and the expression level of Hsp90 is elevated in HCC tumor tissue [15], we hypothesized that ROS might improve Hsp90-driven HBV production. In this research, we exploited cell-free system and HepG2.2.15 cells to test the functional significance of ROS in Hsp90-driven HBV capsid formation. We aimed to determine the effect of oxidative stress on HBV capsid assembly. Our results showed that HBV capsid formation was increased with ROS-induced changes in the conformation of Hsp90 but was decreased by ROS without the Hsp90. Meanwhile, we also found repressive effect of an antioxidant, glutathione (GSH), on HBV capsid formation. Overall, we discovered a previously uncharacterized relation between ROS and Hsp90 and a function of GSH for the Hsp90-drived HBV capsid assembly.

Materials and Methods

Expression and purification of Cp149, p23, B23, and Hsp90

Cp149, p23, nucleophosmin (B23), and Hsp90 were cloned directly using a pET28b vector for Cp149, p23, and Hsp90 (Novagen) and pET21a vector for B23 (Novagen) respectively. All constructs were transformed into BL21 (DE3) + pLysS E.coli (Novagen), and purified and stored with 10% glycerol at -20°C as previously described [9,16].

Analysis of HBV capsid assembly and sucrose density gradient analysis

To study the effect of capsid formation from 20μM Cp149 dimer with several addictive including other proteins (20μM of BSA, B23, Hsp90, p23) and chemicals, such as 0.5mM ATP-r-S (Merck), 2μM geldanamycin (GA, A.G. Scientific, Inc.), 50-200μM hydrogen peroxide (H_2O_2, sigma), 200μM *N*-acetyl-L-cysteine (NAC, sigma) and 1mM GSH (sigma), assembly reaction was conducted in assembly buffer as a previous study [17]. Sucrose density gradient analysis was conducted by ultra-centrifugation as a previous study [9]. Fraction from 1 to 10 (10-50%) was detected by 15% SDS-PAGE using immunoblot analysis with rabbit polyclonal anti-HBV core antibody (Dako).

CD analysis

CD measurements were carried out with a J-815 (Jasco). Spectra were obtained using 1 nm bandwidth, a scan rate of 50nm/min and a response time of 1 s. The quartz cuvette path length was 0.1 cm. The CD measurements were implemented using total protein concentrations of 0.1 mg/ml with 1:1 molar ratio. The solvent was 20mM Tris-

HCl, pH 7.5 without salt, and all CD measurements were performed at 20°C or in 20°C-95°C. Values of a ratio and Tm were measured by SSE software program and denatured protein analysis version 1.01A software program from a J-815 (Jasco).

Quantification of intracellular and extracellular HBV DNA in HepG2.2.15 cells in H_2O_2 treatment

HepG2.2.15 cells were cultured in Dulbecco's Modified Eagle's Medium (DMEM, Welgene) added with 10% fetal bovine serum (FBS, Invitrogen) at 37°C in 5% CO2. Intracellular and extracellular HBV DNA in HepG2.2.15 cells after 12 h of treatment with increasing concentration of H_2O_2 were isolated by phenol–chloroform extraction method, and measured by quantitative PCR (qPCR) using a SYBR-Green reaction mixture (Qiagen) as previously described [9] . The primers, F-5′-GTGTCTGCGGCGTTTTATCA-3′ and R-5′-GACAAACGGGCAACATACCTT-3′, were used to amplify a 98-base pair product from positions 379 to 476 of the HBV genome.

Treatment with inhibitors on HepG2.2.15 cells, and detection of HBV intracellular capsid

HepG2.2.15 cells were treated with chemicals, such as 4μM GA for Hsp90 inhibitor, 30μM buthionine sulfoximine (BS, Santa Cruz Biotechnology Inc.) for inhibitor of glutathione synthesis and 5mM NAC for scavenging H_2O_2. Cells were lysed in lysis buffer containing 50mM Tris–HCl (pH 8.0), 150mM NaCl, 5mM EDTA, and 0.5% NP-40, and centrifuged at 16,000 ×g for 15 min at 4°C to spin down cell debris. Intracellular capsid from the supernatant was separated by electrophoresis on 0.9% agarose gel as a previous study [18] and analyzed by immunoblotting with rabbit polyclonal anti-HBV core antibody (Dako), mouse polyclonal anti-β actin antibody

(Abcam) and rabbit polyclonal anti-Hsp90 antibody (Santa Cruz Biotechnology Inc.).

Statistical analysis

Data of bar graph was expressed as the mean and standard deviation in three independent experiments. The band intensity determined in the ImageMaster 2D Elite software 4.01 (Amersham, Upsala, Sweden). Statistical analysis was performed by SPSS 21.0 software (Chicago, IL, USA) and significance values were set at * $p < 0.05$.

Results

1. ROS increase Hsp90-driven HBV capsid assembly.

Among ROS, H_2O_2 is a relatively mild oxidant and is involved in oxidative stress [19]. In HCC cell lines, H_2O_2 concentration below 300μM have used to investigate the effect of ROS [20,21,22]. To demonstrate that H_2O_2 affects the function of the Hsp90 complex for capsid assembly, the assembly reaction was conducted with Cp149 in increasing concentrations of H_2O_2 in the presence or absence of the Hsp90 complex. Capsid formation was decreased in the presence of only Cp149 but increased in the presence of both Cp149 and the Hsp90 complex with increasing concentrations of H_2O_2 (Fig. 1A), and a ratio of capsid by Cp149 with the Hsp90 complex / capsid by Cp149 at 200μM was the highest (Fig. 1B). Moreover, we determined whether this result was derived specifically from the function of the Hsp90 complex, compared with assembly reaction with nucleophosmin (B23) which also acts as a chaperone and increases HBV capsid assembly [16]. In contrast to the Hsp90 complex, capsid formation was decreased with B23 under H_2O_2 treatment (Fig. 1C). To verify the increase of capsid formation induced by H_2O_2 in the presence of the Hsp90 complex, GA, an inhibitor of Hsp90, was applied with increasing H_2O_2 concentration. Despite the presence of the Hsp90 complex, capsid assembly was decreased with increasing H_2O_2 concentrations with GA treatment (Fig. 1D). Thus, these results show that H_2O_2 promotes Hsp90-driven HBV capsid assembly.

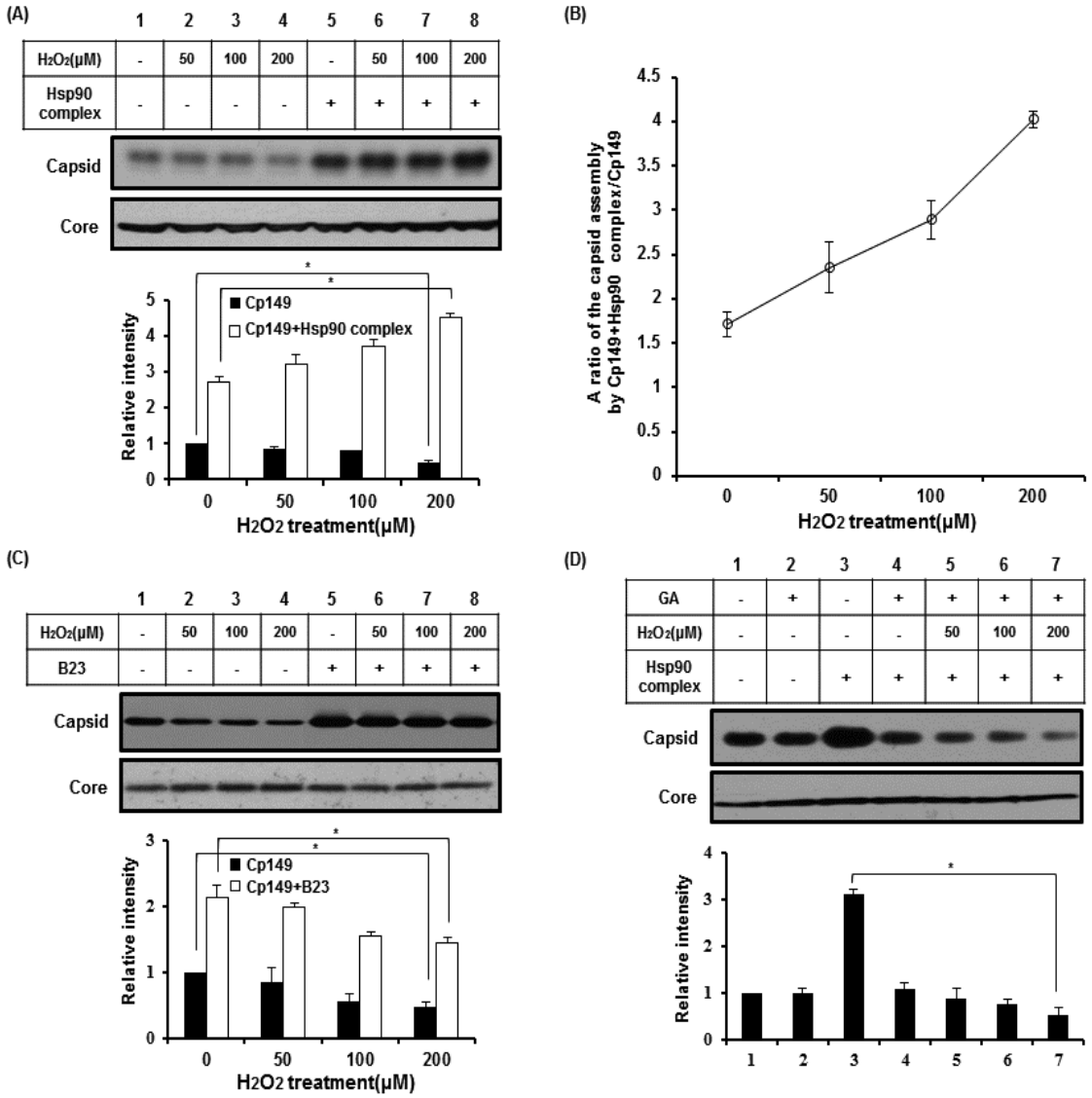

Figure 1. ROS facilitate HBV capsid assembly in the presence of the Hsp90 complex.

(A) For Hsp90 complex formation, 20μM Hsp90 was incubated with 20μM p23 and 0.5mM ATP-r-S for 30 min at 30°C and mixed with 20μM Cp149 dimer in assembly buffer for 30 min at 30°C with increasing concentrations of H_2O_2. (B) A ratio of capsid assembly dependent on the Hsp90 complex was analyzed in experiment for (A). (C)

Increasing concentrations of H_2O_2 were incubated with 20μM B23 and the 20μM Cp149 dimer in same conditions as in (A). (D) 2μM GA was added to Hsp90 with p23 and ATP-r-S for 30 min at 30°C, and this mixture was incubated with Cp149 dimer for 30 min at 30°C with increasing concentrations of H_2O_2. Samples in Fig. 1 were separated by 0.9% native agarose gel electrophoresis, and capsids were detected by immunoblot analysis with an anti-HBV core antibody. Core, the total amount of Cp149, was detected by 15% SDS-PAGE. The graph at the bottom of all gels represents the relative band intensity for each gel. Capsids without any additive were used as a standard (set to 1).

2. Hsp90-driven HBV capsid assembly is increased by ROS pre-treatment at low concentrations.

Because the capsid formation level varied depending on the presence of the Hsp90 complex, we conducted an assembly reaction with Cp149 and the Hsp90 complex to confirm the effect of H_2O_2 applied at different times. We observed the amount of capsids when H_2O_2 was applied to the Hsp90 complex before the assembly reaction with Cp149 (pre-treated H_2O_2) and also when H_2O_2 was applied during the assembly reaction with Cp149 and the Hsp90 complex (post-treated H_2O_2). Capsid assembly was increased with 50μM H_2O_2 in the pre-treatment condition, whereas capsid formation was proportionally increased with increasing concentrations of H_2O_2 in the post-treatment condition (Fig. 2A). Thus, with pre-exposure of the Hsp90 complex to H_2O_2, HBV capsid assembly was increased even at low concentrations of H_2O_2. Furthermore, to confirm the effect of H_2O_2 on facilitating capsid assembly, we performed the assembly reaction using *N*-acetyl-L-cysteine (NAC; sigma), which is a scavenger for H_2O_2, at different times (Fig. 2B). With application of H_2O_2 and NAC together to the Hsp90 complex before the assembly reaction with Cp149 (pre-treated NAC), the amount of capsid did not change when compared to only treatment with NAC but without H_2O_2. However, when NAC was applied when the assembly reaction was conducted with Cp149 and the Hsp90 complex already exposed to H_2O_2 (post-treated NAC), the amount of capsid increased in the H_2O_2 treatment condition more than that in the NAC-only treatment condition without H_2O_2. Thus, these results show that the H_2O_2-treated Hsp90 complex facilitated HBV capsid assembly before NAC treatment.

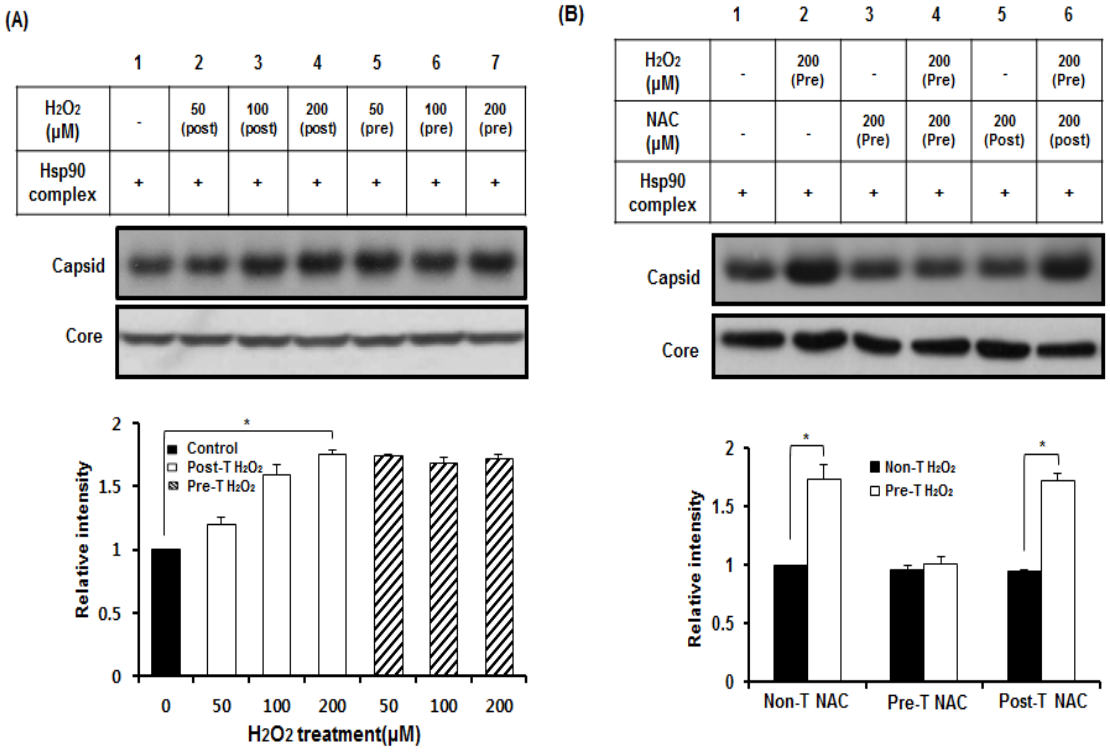

Figure 2. Pre-treatment of the Hsp90 complex with low concentrations of ROS facilitates HBV capsid assembly.

(A) HBV capsid assembly with pre-treated H_2O_2 was compared with that under post-treated H_2O_2, where pre-treated H_2O_2 (Pre-T H_2O_2) was treatment of Hsp90 complexes with H_2O_2 before mixing with the Cp149 dimer and post-treated H_2O_2 (Post-T H_2O_2) was treatment of Hsp90 complexes and Cp149 dimer together with H_2O_2. Lane 1, capsids formed from Hsp90 complex and Cp149 dimer (control); lanes 2–4, capsids formed from Hsp90 complex and Cp149 dimer with post-treated H_2O_2 (0–200μM); lanes 5–7, capsids formed from Hsp90 complex and Cp149 dimer with pre-treated H_2O_2 (0–200μM). (B) These conditions were compared with HBV capsid assembly with pre- and post-treated NAC. Pre-treated NAC (Pre-T NAC) was treatment of Hsp90 complexes with NAC before mixing with the Cp149 dimer. Post-treated NAC (Post-T

NAC) was NAC treatment of the Hsp90 complex and Cp149 dimer together. The H_2O_2 concentration applied to all samples was 200μM and non-T NAC means non-treatment with NAC. Lane 1, capsids formed from Hsp90 complex and Cp149 dimer (control); lane 2, capsids formed from Hsp90 complex and Cp149 dimer with pre-treated H_2O_2; lane 3, capsids formed from Hsp90 complex and Cp149 dimer with pre-treated NAC; lane 4, capsids formed from Hsp90 complex and Cp149 dimer with pre-treated H_2O_2 and pre-treated NAC; lane 5, capsids formed from Hsp90 complex and Cp149 dimer with post-treated NAC; lane 6, capsids formed from Hsp90 complex and Cp149 dimer with pre-treated H_2O_2 and post-treated NAC. All reaction conditions, detection, and analysis for (A) and (B) were the same as those in Fig. 1.

3. GSH inhibits Hsp90-driven HBV capsid assembly.

ROS constitutively induce and activate enzyme glutathione reductase, which produces GSH from GSSG [23]. To test the effect of GSH on Hsp90-driven HBV capsid assembly, we exploited cell-free system. In the reaction of the Hsp90 complex with Cp149, the amount of capsid was decreased by treatment with GSH (Fig. 3A, lane 4). Moreover, with GSH treatment after inhibition of the Hsp90 complex by GA, capsid formation was decreased similarly to capsid formation in the absence of the Hsp90 complex (Fig. 3A, lane 5). Also, BSA (control), Hsp90 complex, and Hsp90 complex with GSH were added to Cp149, and the amount of capsid was assessed over 120 min. In the presence of the Hsp90 complex, GSH treatment resulted in slower capsid formation than only Hsp90-treated capsid formation (Fig. 3B). Moreover, a sucrose density gradient analysis showed that the amount of capsid formed was decreased by GSH with the Hsp90 complex (Fig. 3C-E). Thus, these results show that GSH inhibits the function of Hsp90 in facilitating capsid assembly.

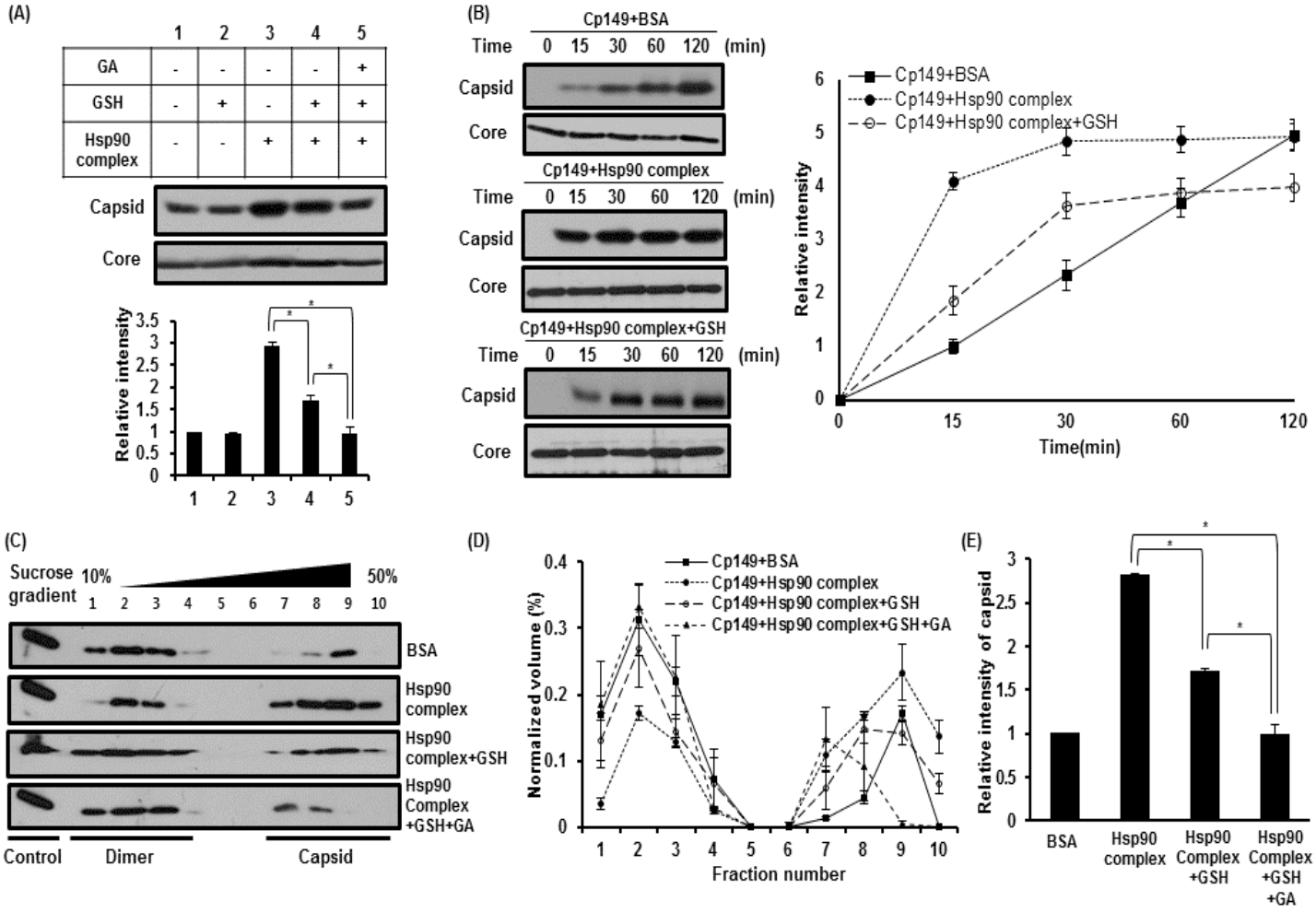
(A)
1 2 3 4 5
GA - - - - +
GSH - + - + +
Hsp90 complex - - + + +
Capsid
Core
Relative intensity
(B)
Cp149+BSA
Time 0 15 30 60 120 (min)
Capsid
Core
Cp149+Hsp90 complex
Time 0 15 30 60 120 (min)
Capsid
Core
Cp149+Hsp90 complex+GSH
Time 0 15 30 60 120 (min)
Capsid
Core
Cp149+BSA
Cp149+Hsp90 complex
Cp149+Hsp90 complex+GSH
Relative intensity
Time(min)
(C)
Sucrose gradient 10% 50%
1 2 3 4 5 6 7 8 9 10
BSA
Hsp90 complex
Hsp90 complex+GSH
Hsp90 Complex +GSH+GA
Control
Dimer
Capsid
(D)
Cp149+BSA
Cp149+Hsp90 complex
Cp149+Hsp90 complex+GSH
Cp149+Hsp90 complex+GSH+GA
Normalized volume (%)
Fraction number
(E)
Relative intensity of capsid
BSA
Hsp90 complex
Hsp90 Complex +GSH
Hsp90 Complex +GSH +GA

Figure 3. GSH inhibits the function of the Hsp90 complex in facilitating HBV capsid assembly.

(A) 20μM Cp149 dimer was independently mixed with the 20μM Hsp90 complex, 1mM GSH, and 2μM GA, and the assembly reaction was performed with these mixtures for 30 min at 30°C. Capsid without any additive (lane 1) was used as a standard (set to 1). (B) Capsid formation was monitored for 120 min after addition of 20μM BSA, Hsp90 complex, and Hsp90 complex with GSH to the Cp149 dimer. The band intensity for capsids with BSA treatment for 15 min was used as a standard and assigned a value of 1. Samples for (A and B) were analyzed as Fig. 1. (C) 20μM Cp149 dimer was mixed with 20μM BSA, Hsp90 complex, Hsp90 complex with 1mM GSH, and GA-treated Hsp90 complex with 1mM GSH independently, and incubated to permit capsid assembly for 30 min at 30°C. With these four samples, a sucrose density analysis was performed. 5% of the total volume of each sample was subjected to immunoblot analysis with an anti-HBV core antibody. (D) The graph shows each band pattern from the fraction of the gel in (C). (E) This graph presents a comparison of each amount of capsid from the sucrose density analysis (fractions 7-10). BSA was used as a control and the amount of capsid after addition of BSA was also given a value of 1.

4. HBV DNA and capsid assembly levels are increased in ROS- and BS-treated HepG2.2.15 cells.

HepG2.2.15 cells derived from HepG2 cells produce HBV particles [24]. To investigate the effect of ROS in HepG2.2.15 cells, HepG2.2.15 cells were treated with an increased concentration of H_2O_2 and *N*-acetyl-L-cysteine (NAC) which is scavenger for H_2O_2. The level of extracellular and intracellular HBV DNA and capsid in HepG2.2.15 cells was increased by increasing concentration of H_2O_2 but not changed in NAC pre-treatment (Fig. 4A and B). Furthermore, examining that Hsp90 played an important role in this effect, HepG2.2.15 cells were treated with GA and/or H_2O_2. The amount of HBV DNA and capsid was decreased in GA and H_2O_2 co-treated HepG2.2.15 cells in addition to only GA-treated HepG2.2.15 cells (Fig. 4C and D). Also, to test the effect of glutathione as an antioxidant on Hsp90 with regard to the amount of HBV genome and capsid in HepG2.2.15 cells, HepG2.2.15 cells were treated with GA and/or BS. Compared with HepG2.2.15 cells without any additive (control), the level of intracellular and extracellular HBV DNA and capsid increased with BS treatment but decreased with GA and BS co-treatment (Fig. 4E and F). Thus, these results indicate that H_2O_2 and GSH contribute to modulation of HBV capsid formation in HepG2.2.15 cells through Hsp90.

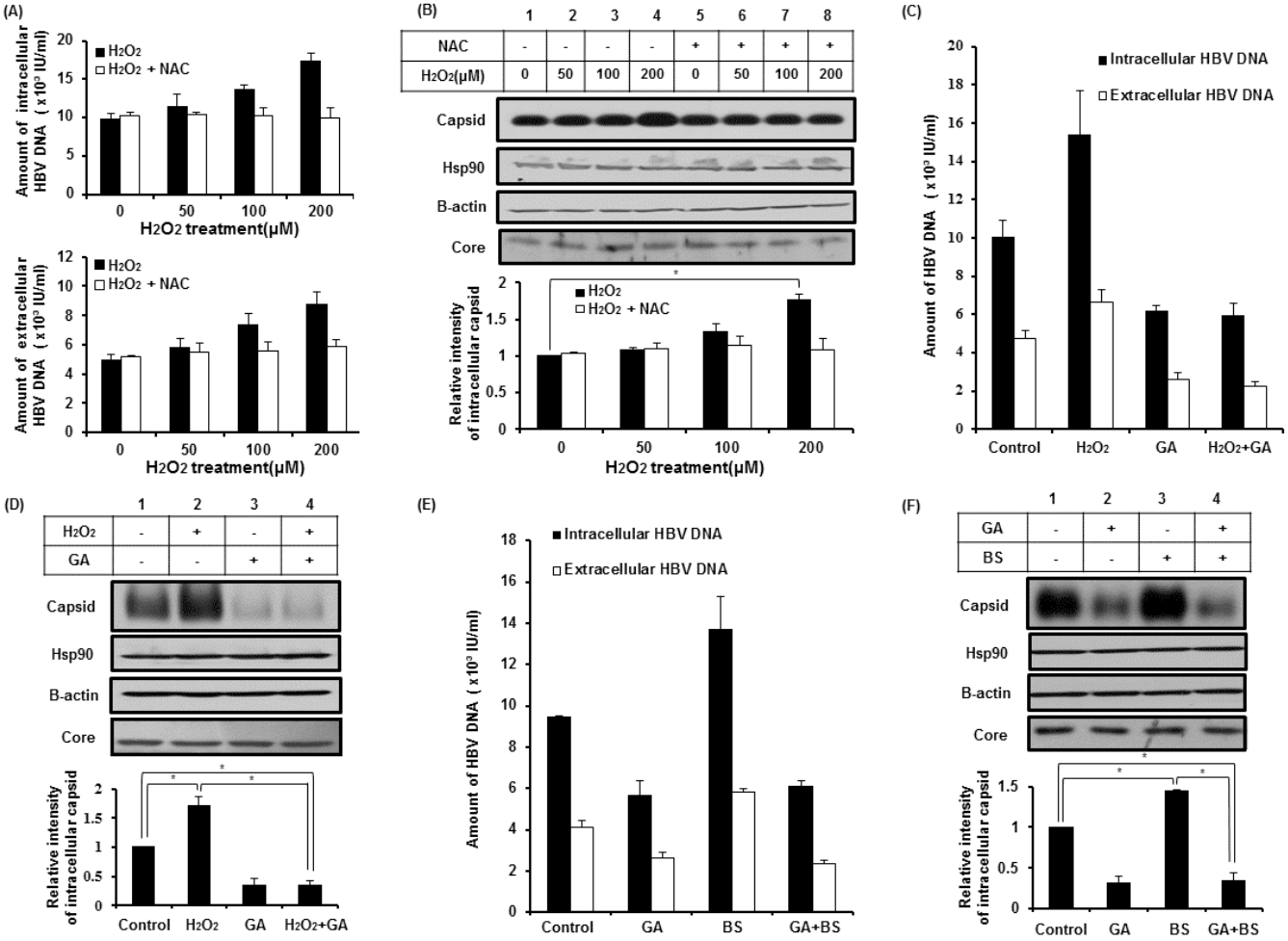
(A)
Amount of intracellular HBV DNA (x10³ IU/ml)
H2O2
H2O2 + NAC
H2O2 treatment(μM)
Amount of extracellular HBV DNA (x10³ IU/ml)
(B)
NAC
H2O2(μM)
Capsid
Hsp90
B-actin
Core
Relative intensity of intracellular capsid
(C)
Intracellular HBV DNA
Extracellular HBV DNA
Amount of HBV DNA (x10³ IU/ml)
Control
GA
H2O2+GA
(D)
(E)
BS
GA+BS
(F)

Figure 4. HBV DNA and capsid assembly levels are elevated by BS and increasing concentrations of ROS in HepG2.2.15 cells.

(A) HepG2.2.15 cells were pretreated with 5mM NAC for 1 h before treatment with H_2O_2, and then increasing concentrations of H_2O_2, 50 to 200μM, were applied for 12 h. Intracellular and extracellular HBV DNA were measured by qPCR in HepG2.2.15 cells and media. (B) HepG2.2.15 cells were treated with H_2O_2 and NAC as in (A) and analyzed by 0.9% agarose electrophoresis for HBV capsid detection. (C) HepG2.2.15 cells were treated with 4μM GA and/or 200μM H_2O_2. The cells were pretreated with 4μM GA for 24 h before H_2O_2 treatment, and then 200μM H_2O_2 were treated in the cells for 12 h. Intracellular and extracellular HBV DNA levels were quantified by qPCR. (D) The same conditions as in (C) were applied to HepG2.2.15 cells and analyzed by immunoblotting of a 0.9% agarose gel for capsids (E) HepG2.2.15 cells were treated with 4μM GA and/or 30μM BS for 24 h, and extracellular and intracellular HBV DNA levels were measured by qPCR. (F) 4μM GA and/or 30μM BS was applied to HepG2.2.15 cells for 24 h, and HBV capsids were analyzed in a 0.9% native agarose gel using immunoblot analysis. Hsp90, β-actin, and core protein in Fig.4 were detected by immunoblot analysis after separation by 12% SDS-PAGE. B-actin was used as a control.

5. ROS and GSH induce conformation change of Hsp90 complex.

To demonstrate the conformation change of the Hsp90 complex by H_2O_2 and GSH, the conformations of the Hsp90 complex were examined by CD analysis. The Hsp90 complex showed spectra typical of helix-containing proteins, with a negative peak at 208 nm and 220 nm and a positive peak at 195 nm (Fig. 5A and B, trace A) [25]. H_2O_2 treatment of the Hsp90 complex resulted in a slight change in shape of the spectrum with a 10% decreased α-helix ratio (Fig. 5A and Table. 1). This spectral pattern for the conformation change was similar to that in a previous study showing conformation changes in Hsp90 caused by ATP [26]. Moreover, we observed that GSH treatment increased the ratio of the α-helix by 16.1% in the Hsp90 complex (Fig. 5B and Table. 1). To investigate the effect of H_2O_2 and GSH on Hsp90-driven capsid stability, we examined the change of CD spectrum in 220nm with increasing temperature, 20°C to 95°C. Among the capsid with non-, GSH-, and H_2O_2-treated Hsp90 complex, capsid with H_2O_2-treated Hsp90 complex started to denature at the highest temperature, and a Tm value for capsid with H_2O_2-treated Hsp90 complex was the highest (Fig. 5C and Table. 2). These results suggest that H_2O_2 induces the conformation change in the Hsp90 complex and finally resulted in the increased stability of the capsid.

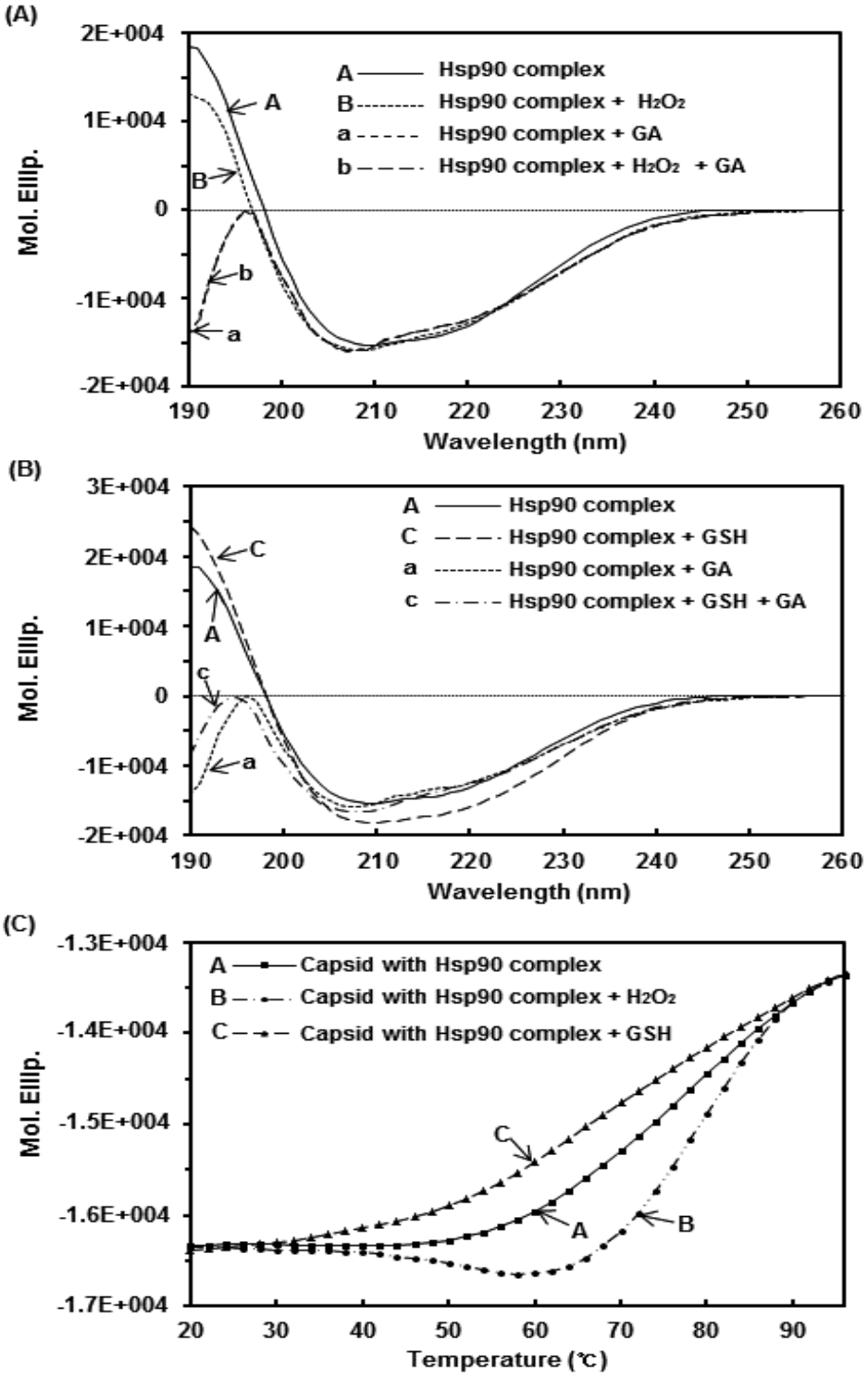
(A)
2E+004
1E+004
0
-1E+004
-2E+004
Mol. Ellip.
190
200
210
220
230
240
250
260
Wavelength (nm)
A Hsp90 complex
B Hsp90 complex + H2O2
a Hsp90 complex + GA
b Hsp90 complex + H2O2 + GA
A
B
b
a
(B)
3E+004
2E+004
1E+004
0
-1E+004
-2E+004
Mol. Ellip.
190
200
210
220
230
240
250
260
Wavelength (nm)
A Hsp90 complex
C Hsp90 complex + GSH
a Hsp90 complex + GA
c Hsp90 complex + GSH + GA
C
A
c
a
(C)
-1.3E+004
-1.4E+004
-1.5E+004
-1.6E+004
-1.7E+004
Mol. Ellip.
20
30
40
50
60
70
80
90
Temperature (℃)
A Capsid with Hsp90 complex
B Capsid with Hsp90 complex + H2O2
C Capsid with Hsp90 complex + GSH
C
A
B

Figure 5. Conformation of Hsp90 complex is changed by ROS and GSH.

(A) All the samples were analyzed by CD in 20mM Tris-HCl pH 7.5 with Hsp90 complex with 200μM H_2O_2 and/or 2μM GA. Spectra were obtained using a 1 nm bandwidth, a scan rate of 50 nm/min, and a response time of 1 s. Trace A, Hsp90 complex alone; trace B, H_2O_2-treated Hsp90 complex; trace a, GA-treated Hsp90 complex; trace b, GA-treated Hsp90 complex with H_2O_2. (B) All condition for analysis was the same with (A). Trace A, Hsp90 complex alone; trace C, 1mM GSH-treated Hsp90 complex; trace a, GA-treated Hsp90 complex; trace c, GA-treated Hsp90 complex with 1mM GSH. The ratio of secondary structure in the Hsp90 complex was shown in Table 1. (C) Changes in molar ellipticity of capsid with H_2O_2-treated, GSH-treated and non-treated Hsp90 complex with elevating temperature in 220nm. CD spectra of samples were recorded as temperature was increased. All samples were subjected to heat treatment in 20mM Tris-HCl pH7.5 in 20°C to 95°C. Spectra were obtained using a 1 nm bandwidth, a temperature slope of 5°C/min, and a response time of 1 s. The values of Tm are listed in Table 2.

Table. 1. Estimation of secondary structure in Hsp90 complex

Reaction Components	A-helix (%)	B-sheet (%)	Turn (%)	Random (%)
Hsp90 complex	15.5	44.5	3.7	36.3
Hsp90 complex + H_2O_2	14.1	41.6	6.3	38
Hsp90 complex + GA	11	42	15.4	31.6
Hsp90 complex + GA + H_2O_2	11	42.1	15.4	31.5
Hsp90 complex + GSH	18	40.6	3.7	37.7
Hsp90 complex + GA + GSH	9.5	47.2	10.7	32.7

A result of CD analysis in Fig 5 A and B was used for estimation of secondary structure in Hsp90 complex in SSE software program. A ratio of α-helix, β-sheet, turn, and random coil was measured and the sum of each ratio for one sample is 100%.

Table. 2. Calculation of Tm values

Reaction Components	Tm (℃)
(A) Cp149+Hsp90 complex	68.98±0.261628
(B) Cp149+Hsp90 complex + H_2O_2	74.42±0.419307
(C) Cp149+Hsp90 complex + GSH	59.18±0.153448

Tm Values for capsid with only Hsp90 complex, H_2O_2-treated Hsp90 complex, and GSH-treated Hsp90 complex were measured for Fig. 5C in denatured protein analysis version 1.01A software program. Tm, midpoint of the thermal transition

Discussion

In HBV capsid assembly, we discovered an effect of H_2O_2 on the Hsp90 complex for HBV capsid assembly, which was increased by 67%, 71% in cell-free system in addition to cell culture system respectively (Fig. 1 and 4). However, capsid assembly was not increased by H_2O_2 in the Hsp90 complex treated by GA, which induces conformation change of Hsp90 leading to catalytically inactive form [27]. This result suggests that the only active form of Hsp90 contributes to the increase in capsid formation by H_2O_2. In addition, previous study demonstrated that a decrease of HBV particle by GA in HepG2.2.15 cells was derived from the result of inhibition of HBV capsid formation [9]. Therefore a decrease of HBV capsid formation by GA with H_2O_2 means that H_2O_2 facilitates HBV capsid formation via Hsp90. Together with a previous study showing that Hsp90 interacted with the HBV core protein and HBV Pol [9,28,29], extensive research is necessary to understand the process of HBV replication by H_2O_2 via Hsp90.

Virus infection is associated with GSH and ROS. Previous studies have shown that cultured cells infected with Sendai virus, HIV, influenza virus, or HCV have decreased intracellular GSH levels, resulting in increasing ROS levels [3,30,31,32,33]. Our results showed that GSH decreased HBV capsid assembly by 42% (Fig. 3). Moreover, in HepG2.2.15 cells, HBV capsid assembly was increased by 44% after BS treatment but decreased by 66% after treatment with both BS and GA (Fig. 4). This result indicates that GSH contributes to reduced production of HBV particles through Hsp90. Previous report showed that GSH levels were significantly low from HBV infection at the beginning of the disease [34]. Low GSH and high ROS level following HBV infection may cause to facilitate HBV capsid assembly. Therefore, we suggest that HBV capsid assembly is dependent on cellular redox state.

H_2O_2 oxidizes cysteine sulfhydryl groups to several oxidized forms such as disulfide bonds [19] and GSH reduces disulfide bonds as an electron donor [19,35,36]. Therefore, we assumed that H_2O_2 and GSH induced conformation changes in the Hsp90 complex. CD analysis data showed that GA treatment induced a decrease in the ratio of α-helices of the Hsp90 complex as H_2O_2 treatment (Fig. 5), indicating that H_2O_2 might induce conformation changes of the Hsp90 complex in favor of capsid assembly with stability regardless of a variation of the ratio of α-helices for that. Thus, we suggest that changes of disulfide formation on the Hsp90 complex may lead to the increase or decrease of HBV capsid assembly.

Our findings have a practical ramification for the better understanding of improved production of HBV by ROS. When taken together, our results demonstrated that a cooperative effect of ROS and Hsp90 through ROS-induced Hsp90 conformation change is a critical event during the process of HBV production. Given that capsid assembly is crucial for completion of the HBV life cycle, an increase of HBV capsid assembly by ROS is important for virus production. Furthermore, our findings also show repressive effect of HBV capsid assembly caused by antioxidant, GSH. Further studies are needed to understand how the ROS-Hsp90 partnership are related to the development of HCC, and testing compounds that block ROS production may be a novel approach for minimizing the generation of HBV particles.

References

[1] J.J. Ott, G.A. Stevens, J. Groeger, S.T. Wiersma, Global epidemiology of hepatitis B virus infection: new estimates of age-specific HBsAg seroprevalence and endemicity, Vaccine 30 (2012) 2212-2219.

[2] A.J. Zuckerman, More than third of world's population has been infected with hepatitis B virus, BMJ 318 (1999) 1213.

[3] K.B. Schwarz, Oxidative stress during viral infection: a review, Free Radic Biol Med 21 (1996) 641-649.

[4] T. Severi, C. Ying, J.R. Vermeesch, D. Cassiman, L. Cnops, C. Verslype, J. Fevery, L. Arckens, J. Neyts, J.F. van Pelt, Hepatitis B virus replication causes oxidative stress in HepAD38 liver cells, Mol Cell Biochem 290 (2006) 79-85.

[5] Y.I. Lee, J.M. Hwang, J.H. Im, N.S. Kim, D.G. Kim, D.Y. Yu, H.B. Moon, S.K. Park, Human hepatitis B virus-X protein alters mitochondrial function and physiology in human liver cells, J Biol Chem 279 (2004) 15460-15471.

[6] C. Seeger, W.S. Mason, Hepatitis B virus biology, Microbiol Mol Biol Rev 64 (2000) 51-68.

[7] W.S. Mason, M.S. Halpern, J.M. England, G. Seal, J. Egan, L. Coates, C. Aldrich, J. Summers, Experimental transmission of duck hepatitis B virus, Virology 131 (1983) 375-384.

[8] W. Sullivan, B. Stensgard, G. Caucutt, B. Bartha, N. McMahon, E.S. Alnemri, G. Litwack, D. Toft, Nucleotides and two functional states of hsp90, J Biol Chem 272 (1997) 8007-8012.

[9] H.Y. Shim, X. Quan, Y.S. Yi, G. Jung, Heat shock protein 90 facilitates formation of the HBV capsid via interacting with the HBV core protein dimers, Virology 410 (2011) 161-169.

[10] J.E. Whittier, Y. Xiong, M.C. Rechsteiner, T.C. Squier, Hsp90 enhances degradation of oxidized calmodulin by the 20 S proteasome, J Biol Chem 279 (2004) 46135-46142.

[11] M.L. Urso, P.M. Clarkson, Oxidative stress, exercise, and antioxidant supplementation, Toxicology 189 (2003) 41-54.

[12] P. Storz, Reactive oxygen species in tumor progression, Front Biosci 10 (2005) 1881-1896.

[13] M. Marra, I.M. Sordelli, A. Lombardi, M. Lamberti, L. Tarantino, A. Giudice, P. Stiuso, A. Abbruzzese, R. Sperlongano, M. Accardo, M. Agresti, M. Caraglia, P. Sperlongano, Molecular targets and oxidative stress biomarkers in hepatocellular carcinoma: an overview, J Transl Med 9 (2011) 171.

[14] A. Ayub, U.A. Ashfaq, A. Haque, HBV induced HCC: major risk factors from genetic to molecular level, Biomed Res Int 2013 (2013) 810461.

[15] S.O. Lim, S.J. Park, W. Kim, S.G. Park, H.J. Kim, Y.I. Kim, T.S. Sohn, J.H. Noh, G. Jung, Proteome analysis of hepatocellular carcinoma, Biochem Biophys Res Commun 291 (2002) 1031-1037.

[16] H. Jeong, M.H. Cho, S.G. Park, G. Jung, Interaction between nucleophosmin and HBV core protein increases HBV capsid assembly, FEBS Lett 588 (2014) 851-858.

[17] H.Y. Kang, S. Lee, S.G. Park, J. Yu, Y. Kim, G. Jung, Phosphorylation of hepatitis B virus Cp at Ser87 facilitates core assembly, Biochem J 398 (2006) 311-317.

[18] S.G. Park, S.M. Lee, G. Jung, Antisense oligodeoxynucleotides targeted against molecular chaperonin Hsp60 block human hepatitis B virus replication, J Biol Chem 278 (2003) 39851-39857.

[19] J.A. Thomas, R.J. Mallis, Aging and oxidation of reactive protein sulfhydryls, Exp Gerontol 36 (2001) 1519-1526.

[20] S.O. Lim, J.M. Gu, M.S. Kim, H.S. Kim, Y.N. Park, C.K. Park, J.W. Cho, Y.M. Park,

G. Jung, Epigenetic changes induced by reactive oxygen species in hepatocellular carcinoma: methylation of the E-cadherin promoter, Gastroenterology 135 (2008) 2128-2140, 2140 e2121-2128.

[21] H.S. Kim, G. Jung, Reactive oxygen species increase HEPN1 expression via activation of the XBP1 transcription factor, FEBS Lett 588 (2014) 4413-4421.

[22] H.S. Kim, G. Jung, Notch1 increases Snail expression under high reactive oxygen species conditions in hepatocellular carcinoma cells, Free Radic Res 48 (2014) 806-813.

[23] O. Zitka, S. Skalickova, J. Gumulec, M. Masarik, V. Adam, J. Hubalek, L. Trnkova, J. Kruseova, T. Eckschlager, R. Kizek, Redox status expressed as GSH:GSSG ratio as a marker for oxidative stress in paediatric tumour patients, Oncol Lett 4 (2012) 1247-1253.

[24] M.A. Sells, A.Z. Zelent, M. Shvartsman, G. Acs, Replicative intermediates of hepatitis B virus in HepG2 cells that produce infectious virions, J Virol 62 (1988) 2836-2844.

[25] D.H. Chin, R.W. Woody, C.A. Rohl, R.L. Baldwin, Circular dichroism spectra of short, fixed-nucleus alanine helices, Proc Natl Acad Sci U S A 99 (2002) 15416-15421.

[26] P. Csermely, J. Kajtar, M. Hollosi, G. Jalsovszky, S. Holly, C.R. Kahn, P. Gergely, Jr., C. Soti, K. Mihaly, J. Somogyi, ATP induces a conformational change of the 90-kDa heat shock protein (hsp90), J Biol Chem 268 (1993) 1901-1907.

[27] C. Prodromou, The 'active life' of Hsp90 complexes, Biochim Biophys Acta 1823 (2012) 614-623.

[28] L. Lott, B. Beames, L. Notvall, R.E. Lanford, Interaction between hepatitis B virus core protein and reverse transcriptase, J Virol 74 (2000) 11479-11489.

[29] M. Nassal, Hepatitis B viruses: reverse transcription a different way, Virus Res 134 (2008) 235-249.

[30] M.R. Ciriolo, A.T. Palamara, S. Incerpi, E. Lafavia, M.C. Bue, P. De Vito, E. Garaci, G. Rotilio, Loss of GSH, oxidative stress, and decrease of intracellular pH as sequential steps in viral infection, J Biol Chem 272 (1997) 2700-2708.

[31] M. Garland, W.W. Fawzi, Antioxidants and progression of human immunodeficiency virus (HIV) disease, Nutrition Research 19 (1999) 1259-1276.

[32] M.Y. Abdalla, I.M. Ahmad, D.R. Spitz, W.N. Schmidt, B.E. Britigan, Hepatitis C virus-core and non structural proteins lead to different effects on cellular antioxidant defenses, J Med Virol 76 (2005) 489-497.

[33] J. Cai, Y. Chen, S. Seth, S. Furukawa, R.W. Compans, D.P. Jones, Inhibition of influenza infection by glutathione, Free Radic Biol Med 34 (2003) 928-936.

[34] K. Swietek, J. Juszczyk, Reduced glutathione concentration in erythrocytes of patients with acute and chronic viral hepatitis, J Viral Hepat 4 (1997) 139-141.

[35] S. Chakravarthi, C.E. Jessop, N.J. Bulleid, The role of glutathione in disulphide bond formation and endoplasmic-reticulum-generated oxidative stress, EMBO Rep 7 (2006) 271-275.

[36] A. Pompella, A. Visvikis, A. Paolicchi, V. De Tata, A.F. Casini, The changing faces of glutathione, a cellular protagonist, Biochem Pharmacol 66 (2003) 1499-1503.

국문초록

B형 간염 바이러스는 활성산소를 생성하고, 간암발전과 밀접한 관련이 있다. 축적된 활성산소는 비정상적인 세포를 증식시키고 염색체 변이를 유도하기 때문에 간암으로의 진행에 있어서 중요한 요소이다. 이러한 산화적 스트레스에서, 열 충격 단백질90 과 글루타치온은 산화적 환경으로부터 세포의 방어기작을 담당한다. 열 충격 단백질90은 산화적 스트레스 환경에서 세포의 구성성분들을 보호하고, 글루타치온은 활성산소를 제거하는 항산화물질로서의 역할을 한다. 하지만 산화적 스트레스와 관련된 이러한 분자들이 B형 간염 바이러스의 캡시드 조립과 연관되어 있는지는 아직까지 알려진 바가 없다. 캡시드 조립은 B형 간염 바이러스 입자 패킹에 중요한데, 열 충격 단백질90이 B형 간염 바이러스의 캡시드 조립을 촉진시킨다는 이전연구결과를 근거로 하여, 우리는 활성산소가 열 충격 단백질90을 통해 캡시드 조립을 더욱 촉진시킨다는 사실을 증명하였다. Cell-free 시스템에서, 활성산소는 열 충격 단백질90과 함께 B형 간염 바이러스의 캡시드 형성을 촉진시키지만, 열 충격 단백질90이 없을 때에는 캡시드 형성을 감소시켰다. 게다가 글루타치온은 열 충격 단백질90의 기능을 억제하여 B형 간염 바이러스의 캡시드 조립을 감소시켰다. Cell-free 시스

템에서의 결과와 마찬가지로, 활성산소와 글루타치온의 억제물질인 buthionine sulfoximine (BS)는 HepG2.2.15세포에서 B형 간염 바이러스의 캡시드 형성을 증가시켰다. 이와 같이 우리는 B형 간염 바이러스의 캡시드가 조립되는 동안 활성산소와 열 충격 단백질90은 상호작용을 한다는 사실을 밝혔다.

주요어: B형 간염 바이러스, 캡시드 조립, 끝을 자른 코어 149 단백질, 활성산소, 열 충격 단백질90, 글루타치온

학번: 2012-23060